

Article

Model Uncertainty for Settlement Prediction on Axially Loaded Piles in Hydraulic Fill Built in Marine Environment

Manuel Bueno Aguado ¹, Félix Escolano Sánchez ^{1,*} and Eugenio Sanz Pérez ²

¹ Civil Engineering Department, Construction, Infrastructures and Transportation, Universidad Politécnica de Madrid, 28040 Madrid, Spain; mbueno@proes.es

² Engineering and Morphology of the Land Department, Universidad Politécnica de Madrid, 28040 Madrid, Spain; eugenio.sanz@upm.es

* Correspondence: felix.escolano@upm.es; Tel.: +34-9-1067-4614

Abstract: Model uncertainty is present in many engineering problems but particularly in those involving geotechnical behavior of pile foundation. A wide range of soil conditions together with simplified numerical models makes it a constant necessity to review the accuracy of the predictions. In this paper, the outputs of some seventy (70) pile axially-loaded tests have been reviewed with a classic numerical model to assess pile deformation. Probabilistic approach has been used to quantify uncertainties coming from soil tests, statistic uncertainty and also from the model itself. In this way, a critical review of the prediction method and a way to quantify its uncertainty is presented. The method is intended to be used in a wide range of engineering problems.

Keywords: model uncertainty; reliability; pile settlement; piles in granular soil; base resistance; skin friction; t-z curves



Citation: Bueno Aguado, M.; Escolano Sánchez, F.; Sanz Pérez, E. Model Uncertainty for Settlement Prediction on Axially Loaded Piles in Hydraulic Fill Built in Marine Environment. *J. Mar. Sci. Eng.* **2021**, *9*, 63. <https://doi.org/10.3390/jmse9010063>

Received: 18 December 2020

Accepted: 4 January 2021

Published: 8 January 2021

Publisher's Note: MDPI stays neutral with regard to jurisdictional claims in published maps and institutional affiliations.



Copyright: © 2021 by the authors. Licensee MDPI, Basel, Switzerland. This article is an open access article distributed under the terms and conditions of the Creative Commons Attribution (CC BY) license (<https://creativecommons.org/licenses/by/4.0/>).

1. Introduction

Land reclamations built out of the coast for industrial or housing purposes are nowadays a challenge for designers, since settlements are critical for their correct performance. Engineers have to predict deformations based on models that include uncertain inputs but also the model itself has uncertain parameters. Comparing predictions with actual outputs on large scale tests is a sound way to calibrate a numerical model and to have an insight in its uncertainties.

This time, the authors have the opportunity to study the behavior of a 20 m thick embankment built in a marine environment by hydraulic filling and then densified with vibrocompaction [1–4]. After, the new platform was tested with an extensive soil investigation

In this paper—which is part of a wider research on model geotechnical uncertainty [5,6]—, settlement predictions for isolated piles are compared to pile load test outputs. In this way, a numerical model is calibrated with the factual results, but moreover, the uncertainties of the model are also highlighted using a probabilistic approach. The model is not only assessed for its accuracy in reaching a good mean prediction but also for its dispersion, collated with the observed dispersion on the large-scale tests.

Pile settlement is a relevant issue for some design but also for pile load test interpretation. However, since small displacements are involved, it is a topic in which codes and specialized literature pay usually little attention.

This time the authors have had the opportunity to review sixty-two (62) pile load test on concrete hollow-stemmed flight augered piles, all of them in a very homogeneous soil profile.

Uncertainties present on the soil investigation due to measurement method and stochastic change in soil parameters are studied and quantified [7]. They are defined as a probabilistic function that can be implemented in the prediction model.

Predictions are based on a classic model defined as a discrete elastic pile supported by vertical elastoplastic springs. These springs are defined by the well-known t-z curve method, proposed by the American Petroleum Institute [8].

The model, initially formulated as a deterministic model, accurately predicts the mean settlement but it does not simulate the observed dispersion. So, a probabilistic parameter is introduced to match also that deviation. In this way, model uncertainty is introduced in the prediction.

So, engineers are provided with a useful tool to assess the accuracy and reliability of the numerical model so that settlement predictions and confidence intervals can be consistently formulated.

2. Site Geology

Persian Gulf shoreline is on the edge of the deep sedimentary basin that forms the Arabian Peninsula and is underlain by a considerable thickness of sedimentary rocks. Relatively young deposits of the Dibdibba formation (Upper Miocene to Pleistocene Epochs, approximately 2 to 10 million years old) outcrops at the surface. These deposits are underlain at depth by the Dammam formation (Upper Eocene Epoch, approximately 38 to 42 million years old).

The Dibdibba formation typically consists of siliceous sands and gravels, with varying amounts of silt and some thin clay and gypsum bands. Cementation is only partial and relatively poor, consisting of calcium carbonate and gypsum.

After dredging and removing other recent marine deposits, Dibdibba formation was used to build the land reclamation close to the shoreline. At the same time, that same formation at a depth where the material was dense to very dense was the foundation of the fill.

Therefore, a very thick deposit of granular material, partially natural and partially man-made was generated. The tests described in this paper and the carried out soil investigation affect mainly the hydraulic fill and the upper part of its foundation.

3. Soil Conditions

The ground profile is described as a 20 m thick fill formed by hydraulic methods below water level and by layer compaction above. The fill is founded below the sea level on a natural granular soil profile made of silty sand with a density increasing with depth.

The fill is made of siliceous sands with fine percentage (pass through #200) lower than 20%. The material is described as a well graduated sand or silty sand where the medium-sized predominates. They are mostly rounded, with a silty fraction and sporadically some gravel. The technical specifications of the material used for the filling are summarized in the following Table 1.

Table 1. Table of technical specifications of the filling hydraulic.

| Property | Type 1 |
|------------------------------|--------|
| Maximum particle size | 125 mm |
| Maximum % greater 125 mm | 0 |
| Minimum % passing 2 mm sieve | 35 |
| Maximum % passing 75 micron | 20 |
| Maximum % clay (<2 micron) | 2 |
| Liquid Limit (%) | <35 |
| Plasticity Index (%) | <10 |

The fill was dredged from the seabed nearby, so that natural soil below the fill is also made of this same material

After the discharge, the material was compacted by deep vibrocompaction in a $2.5 \times 2.5 \text{ m}^2$ mesh. The operation is controlled until it is densified up to 90% of its maximum dry density.

On top of the hydraulic fill, an additional 3 m engineering fill was built. It was made of the same granular material but placed by compacted 25 cm-thick layers. On this platform concrete piles were built by augering. The piles were 800 mm diameter and 22 to 28 m long.

Site Investigation Uncertainty

Once vibrocompaction was completed and before piling, it was carried out a soil investigation which includes sixteen (16) boreholes with Standard Penetration Tests (SPT) each meter and about thirty (30) continuous Cone Penetration Test (CPT).

The SPT results (N_{SPT}) are presented in the following Figure 1. SPT indexes have been corrected by hammer energy to achieve a homogeneous value corresponding to N_{60} index and by groundwater, according to the following criterion (Equation (1)) [9–11].

$$\text{If } N_{SPT} > 15 \quad N_{SPT} = 15 + 0.5 \times (N_{SPT} - 15) \tag{1}$$

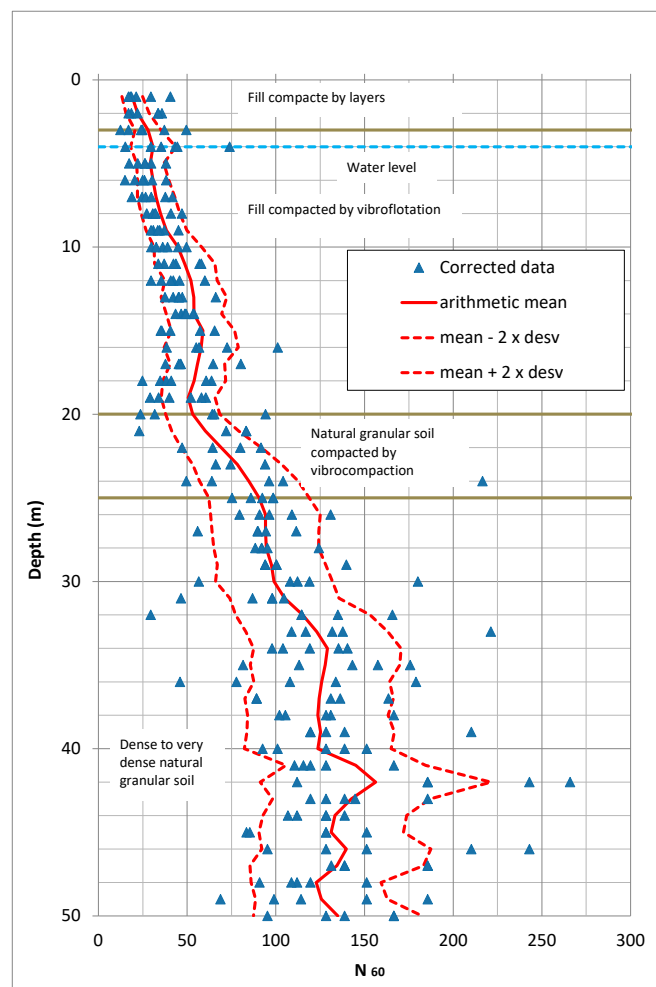


Figure 1. Corrected SPT results.

Engineers are usually surprised by the large dispersion of the outputs, even though they are all carried out on a fairly homogenous material, as it is in this case.

This can be partially attributed to the expected random behavior of the soil. Arguably, the resistance of the soil is a random variable with a certain unknown mean and a certain standard deviation.

Another part of that dispersion is due to the measuring equipment. Including within this concept everything related to the use of different devices, different personnel, variations in the calibration of the equipment over time, etc. These two sources of uncertainty will be dealt with in this section so that they can be statistically quantified.

Firstly, a correction with physical sense is introduced. Variations in vertical resistance that can exist within the same layer are gradual. Abrupt variations are introduced by the measuring equipment. Therefore, the mean value at a point must be influenced by the mean value at the top and bottom levels. Thus, the mean at a certain depth is corrected with the expression (Equation (2)).

$$N_{\text{corrected}, i} = 0.4 \times N_i + 0.2 \times (N_{i-1} + N_{i+1}) + 0.1 \times (N_{i-2} + N_{i+2}) \tag{2}$$

where; N_i is the N_{60} average value at a depth i .

Second correction comes from comparing different type of test. The current site investigation includes also CPT tests carried out on the same level that the SPT boreholes. Comparing the results of each other will be used to precisely correct the measurement uncertainty introduced by the equipment that carries out the SPT tests.

The idea behind is the concept of minimum statistical variance. It is well known that SPT and CPT tests measure different parameters but also that there is a relationship between them [12,13]. This ratio can be obtained by comparing the results of both sets of tests. However, the issue of interest at the moment is the dispersion presented by both tests. It could be said that the lower dispersion is an upper limit of the dispersion of the random variable that represents the resistance of the soil. Thus, the test with the highest dispersion must be corrected to a dispersion similar to that of lower one; this correction being a way to eliminate uncertainty in the result introduced by the measurement test.

The following Figure 2 shows the point resistance measured in CPT tests. From there, the mean (represented in yellow) and the mean \pm the standard deviation (represented in blue) have been obtained for each depth.

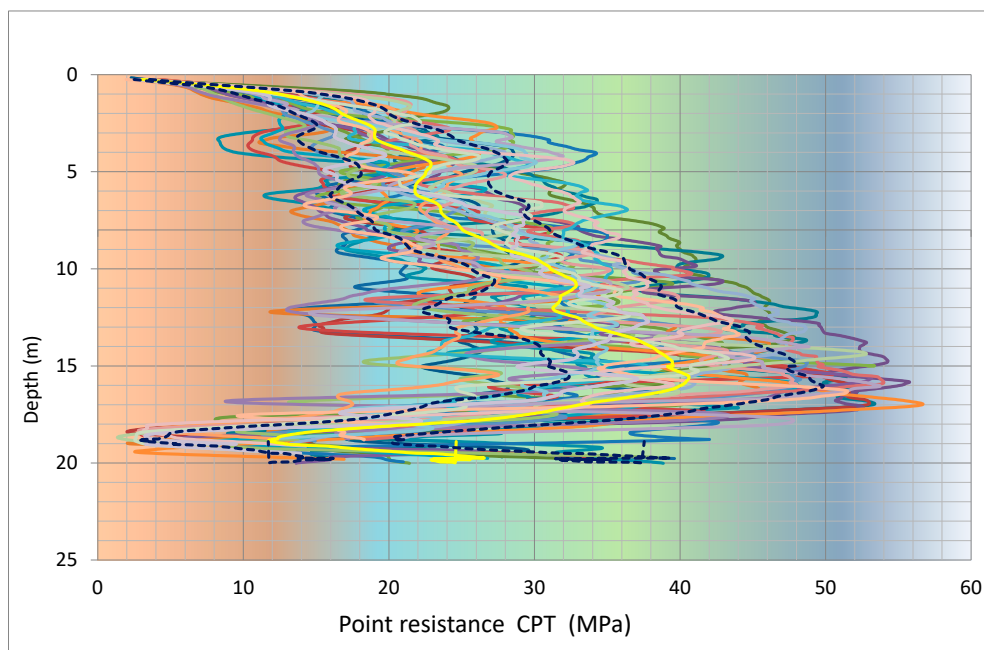


Figure 2. Point resistance CPT results.

In the same way, the mean and standard deviation have been obtained at each depth for the SPT test, based on the data in Figure 1. So, both dispersions can be compared through the ratio defined as (Equation (3)):

$$v = \frac{\text{standard deviation}}{\text{average}} \tag{3}$$

These results are presented in the Figure 3. It is noted that:

- The dispersion on SPT test is higher than that on CPT test, at least in the first 16 m. SPT test dispersion is varied between 0.4 and 0.7, while the CPT dispersion is around 0.2.
- In the last four meters, both dispersions are similar. Their values are in the range of 0.4 to 0.7.

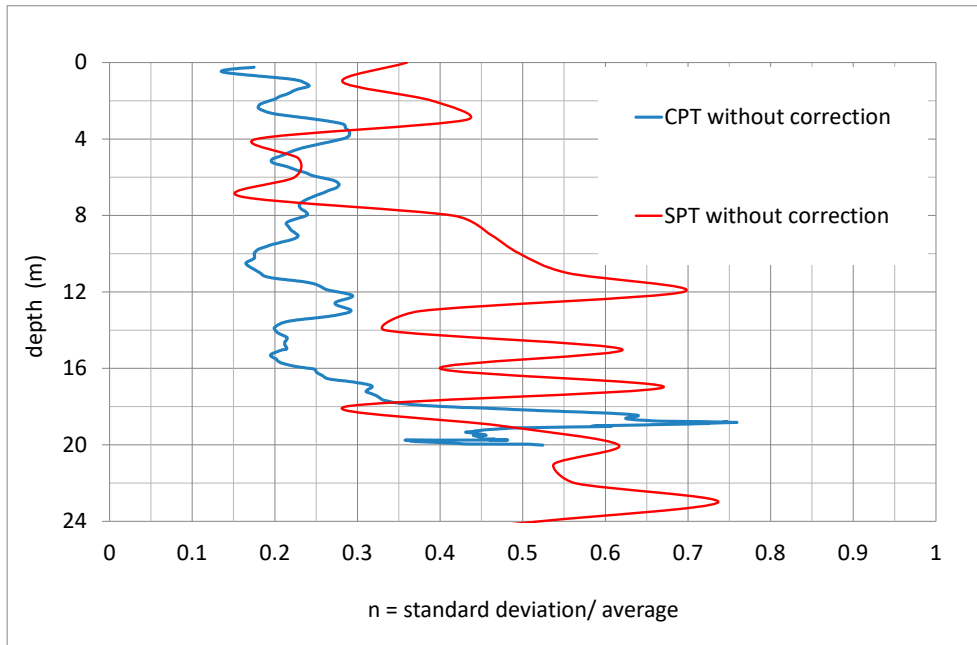


Figure 3. ν -parameter for CPT and SPT.

It can be concluded that the dispersion introduced by the SPT test is at least the difference between the red and blue lines observed in Figure 3.

This observation allows reviewing the SPT original values. It is noted that the dispersion of the soil resistance must be below the parameter 0.2. Therefore, all SPT results that are above or below the mean plus/minus twice the standard deviation have a probability of occurring less than 5%, calculated as follows (Equation (4)):

$$\text{If } \text{ABS}(N_{60} - \mu) > 2 \times \mu \times \nu \text{ then } N_{60} \text{ is removed} \tag{4}$$

Values that exceed this amount are removed from the sample and the mean and standard deviation are calculated again.

Figure 4 shows the new dispersion parameter along with those previously obtained. It is noted that on this occasion the dispersion of the CPT and SPT test are comparable.

Different authors indicate the expected typical variation of a geotechnical parameter within a homogeneous soil layer due to the random variability of its strength. One such reference is ROM [14]. It can be concluded that for the CPT and SPT tests, typical values of ν -parameter are about 0.15.

Since the corrected value of ν -parameter is close enough to the expected random soil strength, it can be consisted that the uncertainty introduced by the measurement method has been taken into account and almost corrected. Applying the two above corrections, it is finally obtained an average and corrected deviation from the SPT test, as it is shown in Figure 5.

Thus, corrections made in SPT test outputs by comparing with CPT and including all the available information allow reducing measurement uncertainty almost completely.

In this case, a large soil investigation is available, so that statistical uncertainty due to the size of the sample can be neglected. If the number of SPT tests were small, a new uncertainty arises due to the lack of a sufficiently large size sample.

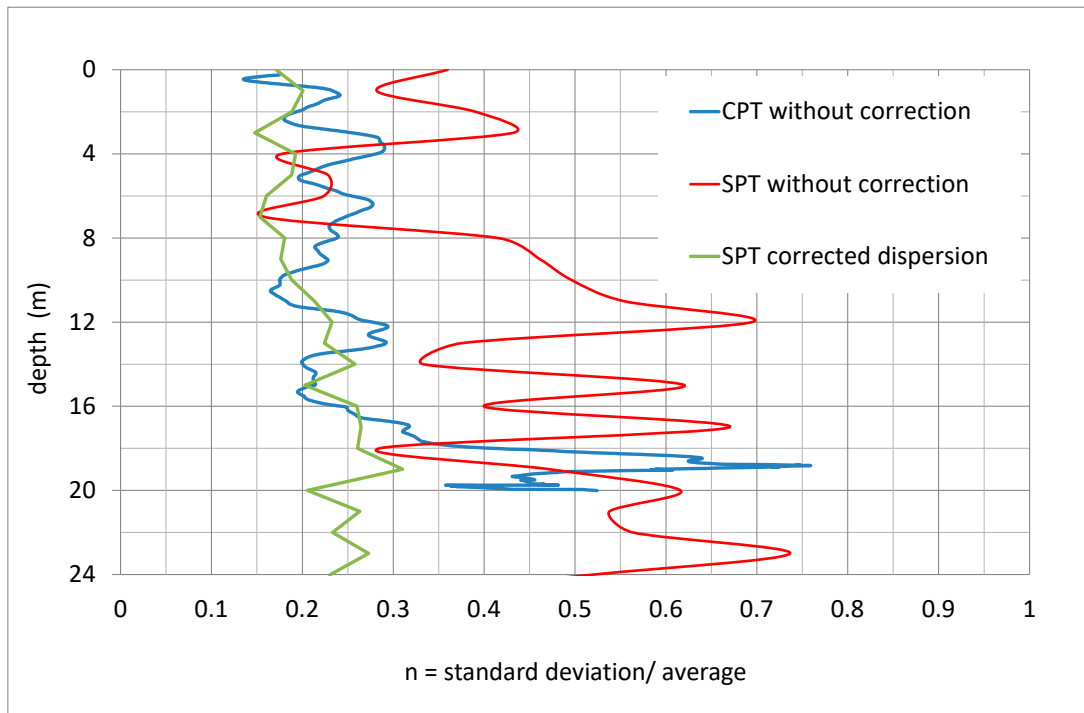


Figure 4. v -parameter for CPT and SPT, including corrected SPT.

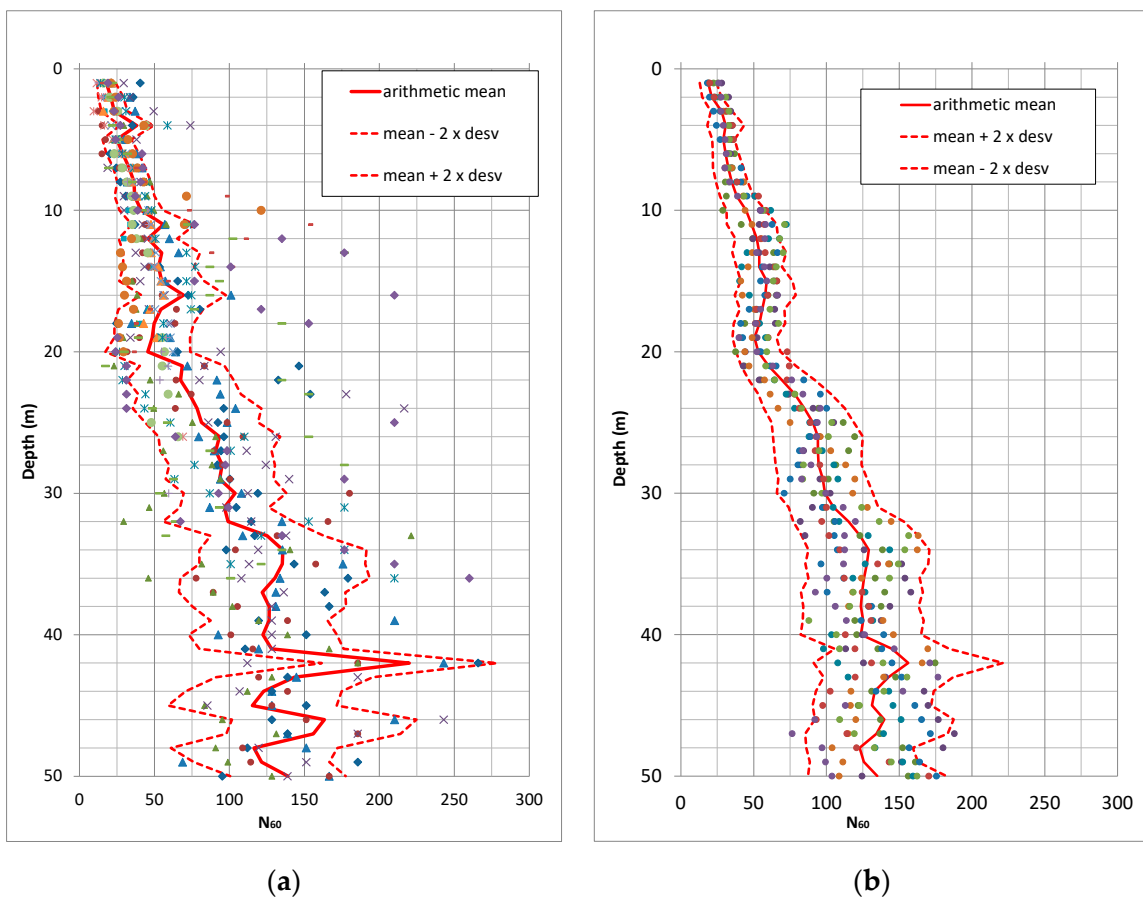


Figure 5. NSPT representation: (a) Example of a statistical representation of the SPT-parameter corrected by method and statistical uncertainty; (b) Artificial SPT profile generated by probabilistic Monte Carlo Method.

4. Pile Analytical Model

A site investigation usually allows stating prediction on pile behavior, as for instance ultimate bearing capacity or load-settlement performance. For granular soil, SPT index can be used to support that prediction, following the procedure below.

SPT index is related to relative density. Gibb & Holtz [15] give a well-known correlation between them and the vertical effective pressure.

1. Relative density is related to the ultimate skin friction and base resistance according to API.
2. The pile can be split in same-length slices. At each slice, an ultimate skin friction is associated depending on its depth. The deepest slice has additionally a base resistance.
3. For each pile slice, it is calculated its t-z curve and for the deepest the base bearing capacity curve, according to the aforementioned code.
4. That analytical model gives a load-settlement prediction curve which later can be compared to the real-scale load test

The following paragraphs describe this procedure in more detail:

4.1. Relative Density from SPT Index

Relative density (DR%) can be obtained from, SPT index according to the Gibb & Holtz formulation. So:

$$DR(\%) = \sqrt{\frac{N_{60}}{23\sigma'_v + 16}} \times 100 \tag{5}$$

where

σ'_v is Vertical effective stress at the SPT test depth.

N_{60} is SPT-index corrected by hammer energy and depth.

$$N_{60} = N_{SPT} \frac{E_r}{60} C_r \tag{6}$$

where

N_{SPT} is the SPT value corrected only by groundwater table.

E_r is the relative hammer energy.

C_r is a factor that accounts for the depth where the test is performed, according to the expression below:

- From borehole top to 3.0 m deep, it is 0.75
- Below 3.0 m deep, $z = 3.0$ m $C_r = (z - 3)/28 + 0.75 < 1.0$

4.2. Ultimate Skin Friction and Base Resistance

For piles in granular soil, skin friction $f(z)$ is a function of relative density and effective pressure. It can be obtained by the expression:

$$f(z) = \beta \times p_0(z) < \tau_{max} \tag{7}$$

where

$p_0(z)$ Vertical effective pressure at z depth.

β : friction factor whose value is a function of the relative density.

$$\beta = 0.8 F \tan(\delta) \tag{8}$$

For hollow tubular driven piles, F-value could be 1.0. For close-end displacement driven piles F-value could be 1.25. For other piles, it is usually recommended to look for experience or specific test.

For ultimate bearing capacity (q) in granular soil. The following expression can be used.

$$q = N_q p_{0,tip} < q_{max} \tag{9}$$

where:

N_q : non-dimensional parameter

$p_{0,tip}$: effective vertical pressure at the base of the pile.

The following charts collect the relationship needed to develop this formulation based on the soil relative density (Figure 6).

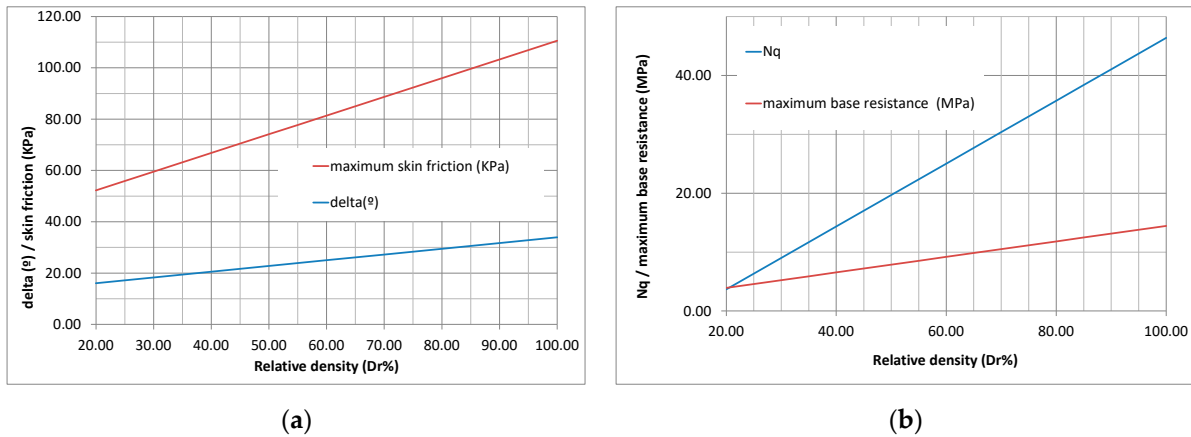


Figure 6. (a) Relationship between relative density and skin friction; (b) Relationship between relative density and resistance.

4.3. Pile Model

Figure 7 shows the pile model used to solve the load-settlement relationship. It consists of splitting the pile in equal-length slices. The slices are united by an elastic spring (K_i). Each of them has a weight (P_i) and ultimate skin friction (Rf_i). The deepest slice has additionally a base resistance (Rp). At pile top, it is applied a load (F_0).

Each slice undergoes an absolute offset (u_i), as a result of the application of the external load and weight. u_i is positive downward. The following equation system solves the mathematical problem.

$$F_0 = Rf_1(u_1) + K_1(u_1 - u_2) - P_1 \tag{10}$$

$$0 = Rf_2(u_2) + K_2(u_2 - u_3) - K_1(u_1 - u_2) - P_2 \tag{11}$$

$$0 = Rf_3(u_3) + K_3(u_3 - u_4) - K_2(u_2 - u_3) - P_3 \tag{12}$$

$$0 = Rf_i(u_i) + K_i(u_i - u_{i+1}) - K_{i-1}(u_{i-1} - u_i) - P_i \tag{13}$$

$$0 = Rp(u_n) + Rf_n(u_n) + K_n(u_n) - K_{n-1}(u_{n-1} - u_n) - P_n \tag{14}$$

K_i is the pile stiffness that takes the value:

$$K_i = \frac{E \times A_i}{L_i}$$

where:

E : pile deformation modulus

A_i pile cross-section area.

L_i : slice length.

The solution of the previous system provides the seeking relationship between applied external pressure F_0 and displacement at the top pile (u_1). Since skin friction $Rf_i(u_i)$ and base resistance $Rp(u_n)$ are functions of displacement, the system is nonlinear and it has to be used an iterative algorithm to reach the solution.

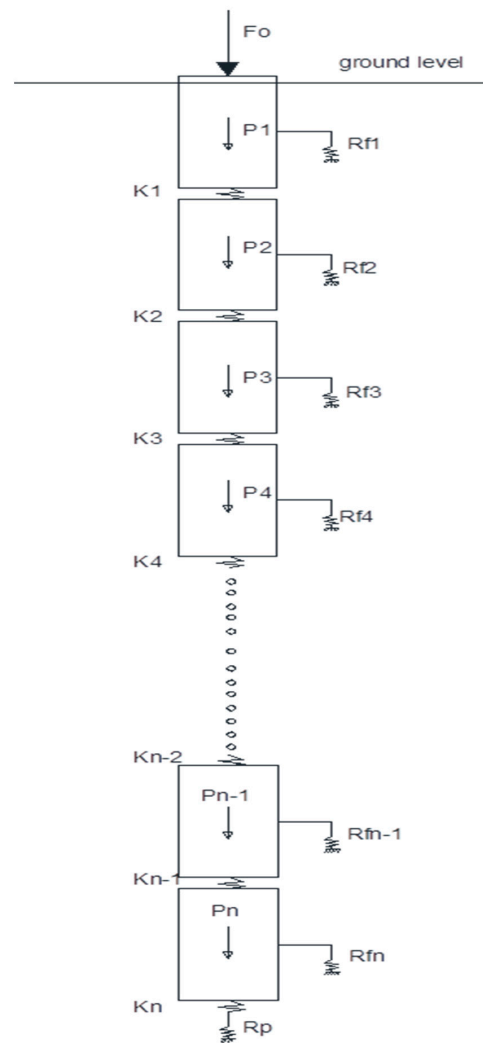


Figure 7. Soil-pile analytical model.

4.4. *t-z Curve and Q-z Curve*

R_{fi} functions are obtained from the t-z curve defined in standard ISO 19901-4:2003 (API RP 2GEO). Base resistance also follows the recommendations of this standard. The following Figure 8 shows the used functions.

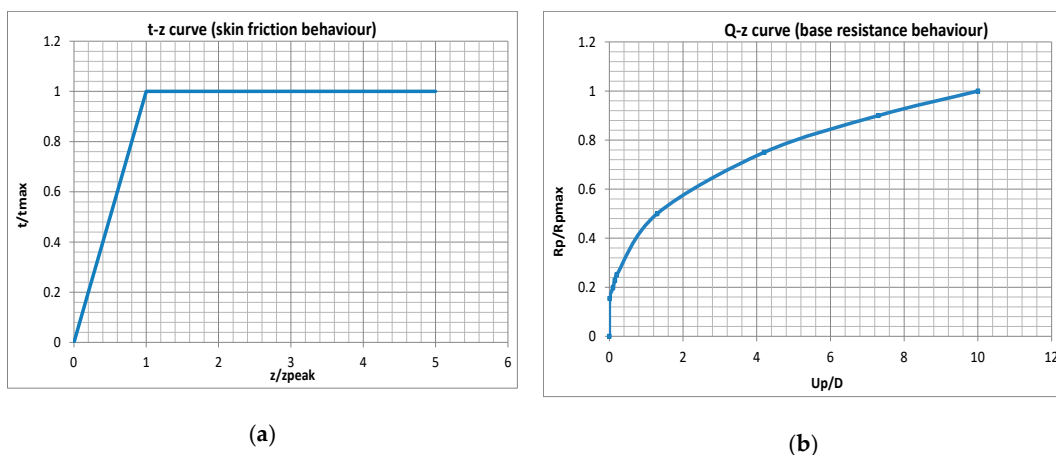


Figure 8. Soil-pile deformation relationship (a): t-z curve; (b): Q-z curve.

4.5. Load Application

The total load F_0 is applied by steps as it is done in the large-scale load test. Positive load is downward. Model admits starting loads as tension (upwards) or compression (downwards).

The weight of the pile is considered through the density of the structural section. If the initial charge is zero the model provides only the settlement due to the weight of the pile.

5. Pile Load Test Outputs

There are sixty-two (62) load tests conducted on 0.8 m diameter concrete piles. The piles were executed by hollow-stemmed flight augering. Pile length ranged between 22 to 28 meters.

The difference in length between the piles is due to the depth where dense sand is located, which is reached by all the piles. Therefore, it can be said that all the piles are supported in a layer of similar mechanical properties.

The piles were tested in a single cycle of loading up to a value of 3.150 KN. Maximum load was reached on five load steps.

The following Figure 9 represents the length of the piles with respect to settlement. The following is observed:

- There is no correlation between the length of the pile and total settlement. This can be explained by the fact that all the piles have been punched to the dense sand layer, so their support conditions are similar.
- The tests with more frequent values are separated from other tests, which are considered special cases and are beyond the average behavior. Four out-of-average pile tests were removed, since it was suspected that their support conditions were different from others

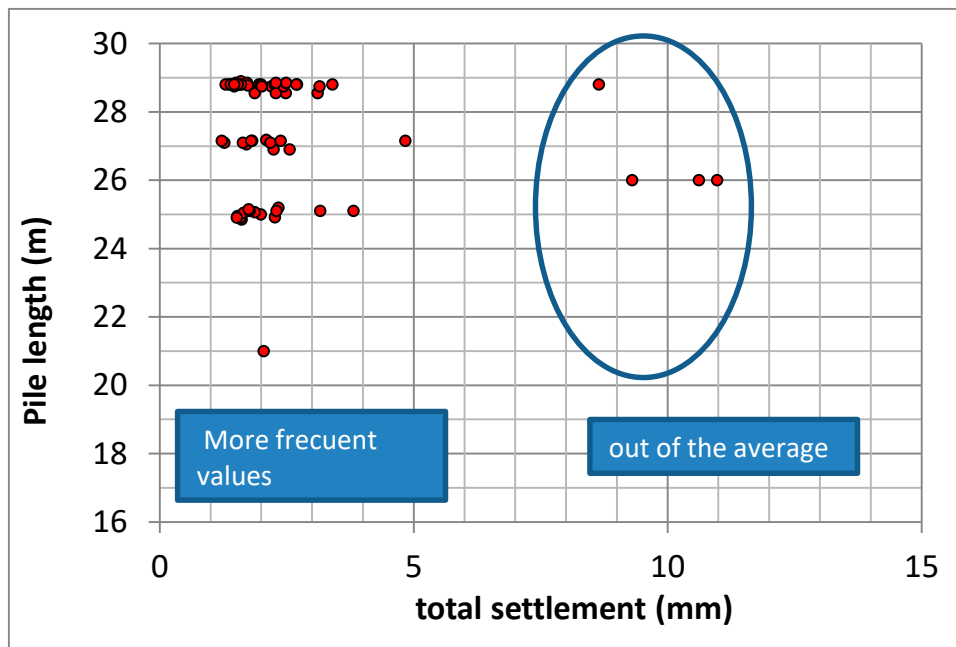


Figure 9. Concrete pile load test outputs.

For the more frequent values, Figure 10 below shows the output distribution and their statistical parameters. Statistical parameters are shown in Table 2.

The following Figure 11 represents an example of some of the more-frequent-value load tests.

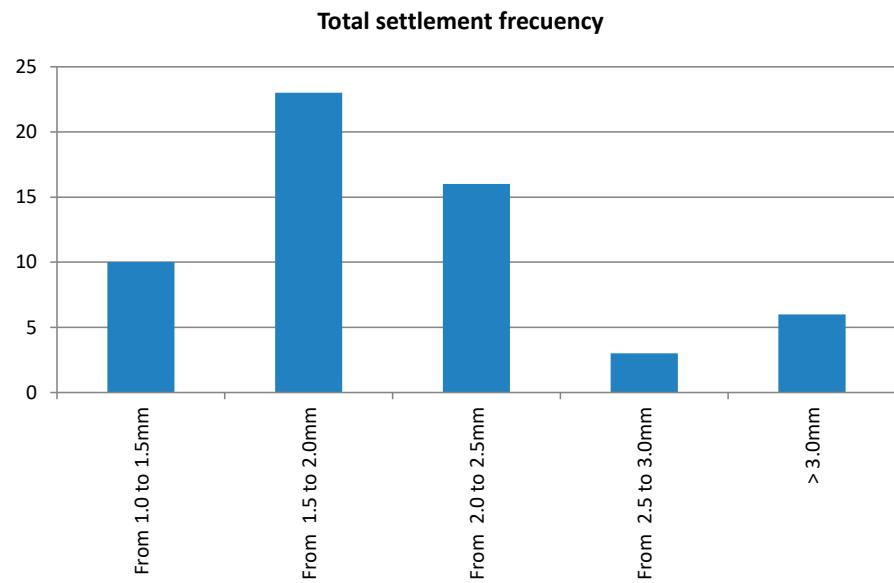


Figure 10. Settlement distribution of concrete load test.

Table 2. Statistical parameter of concrete load tests.

| Settlement | Values |
|--------------------|---------|
| Maximum settlement | 4.84 mm |
| Minimum settlement | 1.22 mm |
| Average | 2.05 mm |
| Standard deviation | 0.68 mm |

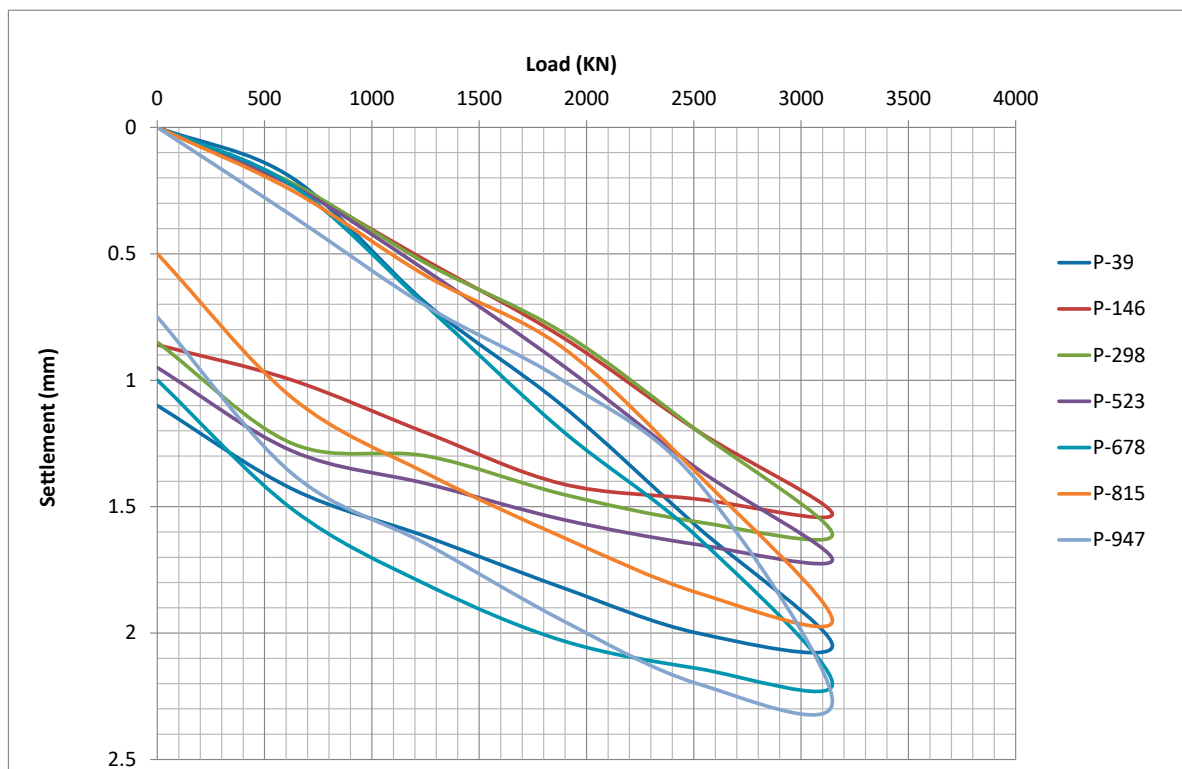


Figure 11. Concrete pile load test—zone 1.

6. Fitting the Analytical Model and Pile Load Test

Pile load tests have been grouped in eight zones and each zone is characterized by a borehole place at that zone. Therefore, eight different soil profiles have been used. Nevertheless, all of them were similar.

To achieve a good fit with these tests, it is necessary to modify some parameters of the model. It was found that the influencing parameters are skin friction and Z_{peak} value.

Other parameters with less influence are: the base resistance, pile stiffness and pile diameter.

The following Figure 12 represents one of the adjustments made for load tests conducted in zone 2. In this case, the adjustment is achieved improving skin friction by 2 and using a Z_{peak} value of 0.17%D.

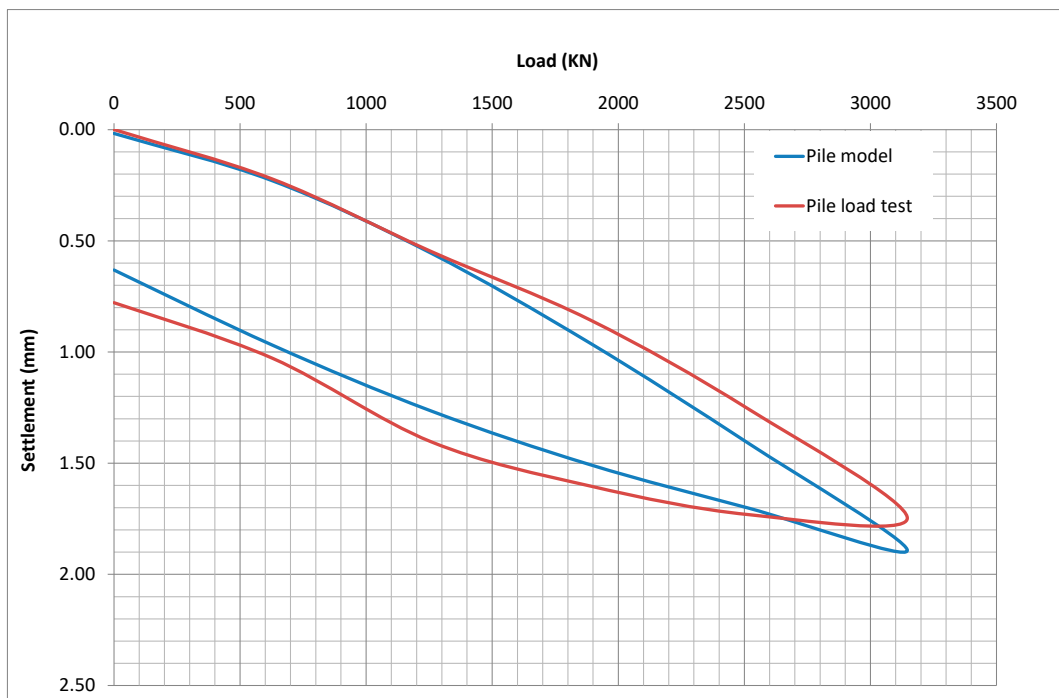
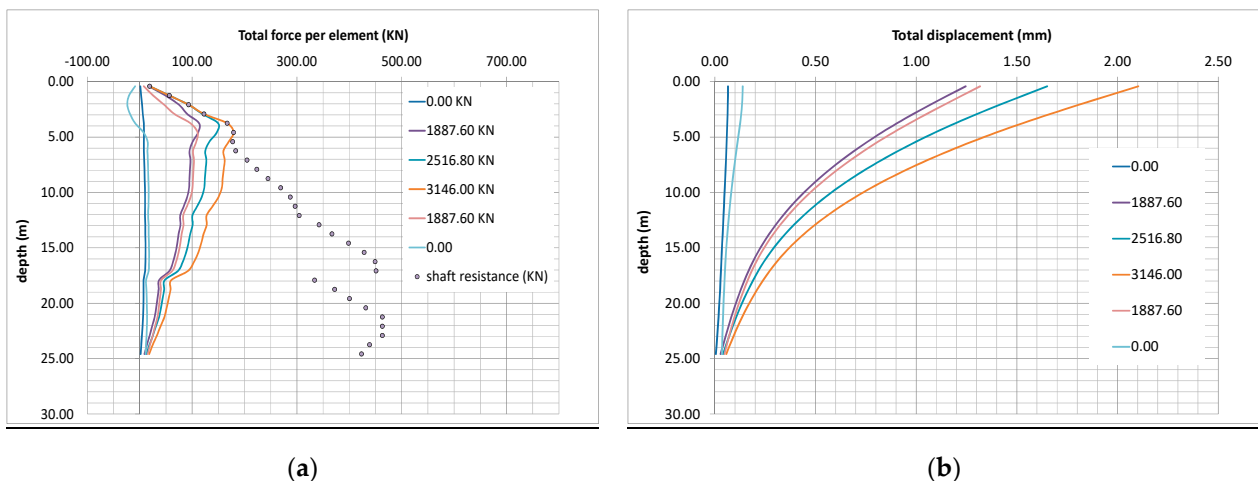


Figure 12. Numerical model and pile load test fitting in zone 1 Concrete pile.

It is represented also for this adjustment the distribution of forces and displacement against depth in Figure 13.



(a)

(b)

Figure 13. Numerical models outputs for each load step (a) skin friction versus depth (b) displacement distribution versus depth.

The following Figure 14 shows the mobilized base resistance. It is shown that the maximum load reached at the base is less than 400 KN, which means that only 10% of the total load of the test is supported by the pile tip.

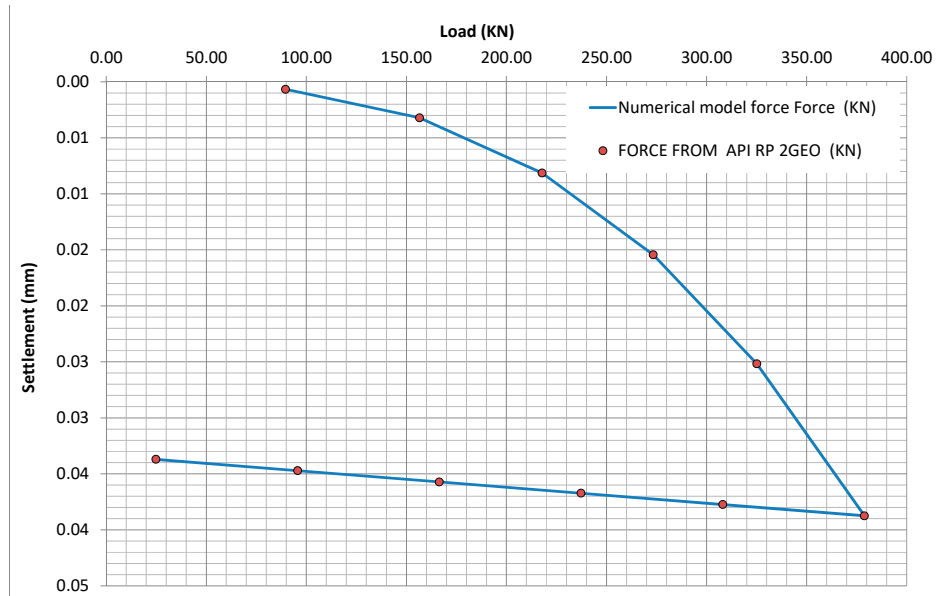


Figure 14. Base resistance. Concrete piles.

The sensitivity of the model against the two main parameters has also been analyzed. The outputs are presented in the following Figure 15. It is noted that for a proper fit, the skin friction has to be multiplied by a factor that is between 2.0 to 2.5.

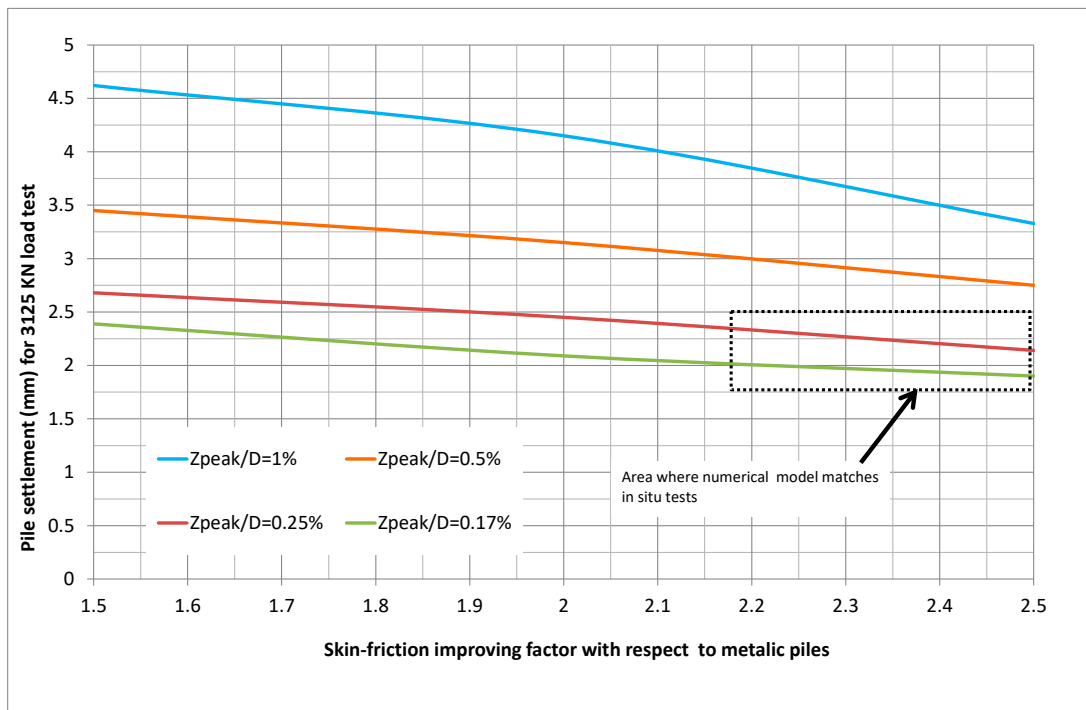


Figure 15. Sensitivity analysis of Zpeak values for concrete piles.

This result is reasonable considering that the basic value is for metal-soil surface and that the tested piles are casted in-situ. The different roughness and bounding of both surfaces is obvious.

In addition to skin friction, the Z_{peak} value has also to be reduced. This value gives the slope of the t-z curve; so that a low value means a rapid mobilization of skin friction, and therefore, for the same level of load, there is less deformation.

7. Probabilistic Approach

The model presented above was tested by a probabilistic approach in order to quantify the uncertainty of the model. The applied methodology is as follows:

1. Artificial soil resistance profiles based on SPT tests are generated, so that they meet the expected mean and standard deviation previously defined at soil conditions section. It has been assumed a Norma Distribution for SPT values.
2. For each of these artificial profiles, pile settlement is calculated using the same load pattern that in the load tests. Total bearing capacity is also calculated.
3. Settlement distribution generated by artificial profile is compared to the pile load test distribution.
4. Both distributions have the same mean, after reasonable and small adjustments are introduced on the model.
5. However, dispersion in the pile load test outputs is larger than in the model. Therefore, it is necessary to introduce a statistical function that takes into account the uncertainty of the model itself.

This procedure and its outputs are described below:

7.1. Artificial Soil Resistance Profiles Generation

Based on the expected mean and standard deviation of soil resistance, artificial profiles are generated. A total of 50 profiles have been used. They are represented in Figure 5b.

7.2. Pile Bearing Capacity

The model requires working out the total bearing capacity in order to define the t-z and base-displacement functions. Since the inputs are statistical functions, the outputs are also given in the same way. The following Figures 16 and 17 show separately the point and shaft resistance of the piles.

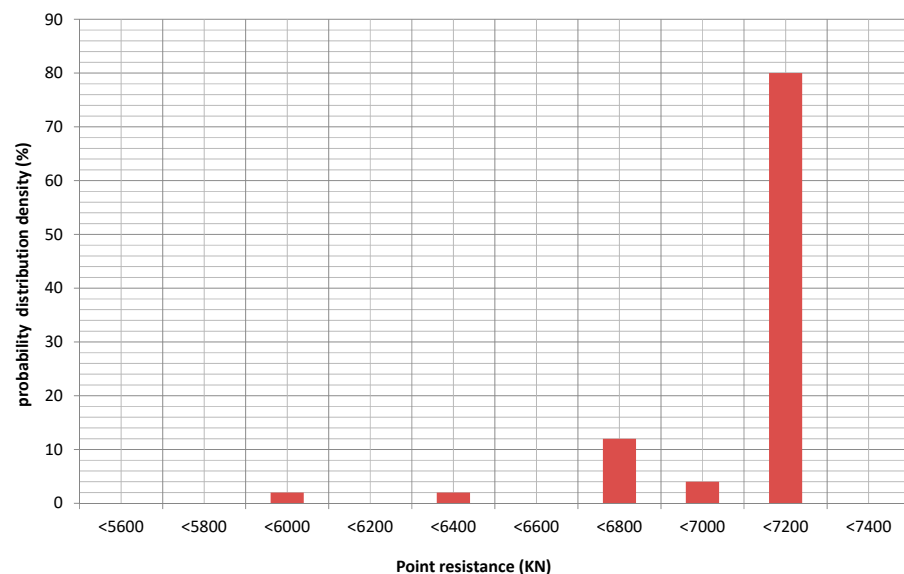


Figure 16. Generated distribution for point resistance.

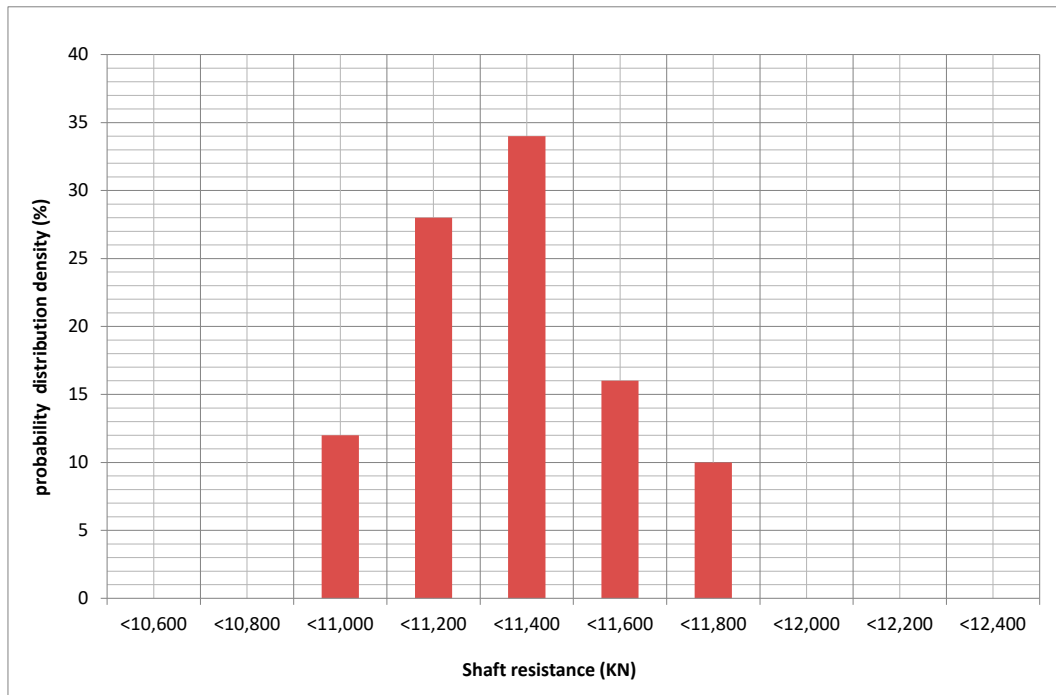


Figure 17. Generated distribution for shaft resistance.

It is noted that:

1. The point resistance is hardly affected by the stochastic variation in soil strength. This result can be explained considering that soil strength and density are related. At the pile tip, density is always at its very high; therefore, base resistance is often taking the maximum value.
2. However, shaft resistance shows a higher dispersion that is related to the dispersion of the input data.

7.3. Pile Settlement Calculation

The model provides the pile settlement. The settlement is also a probability distribution function. Figure 18 below compares it with the pile load test distribution.

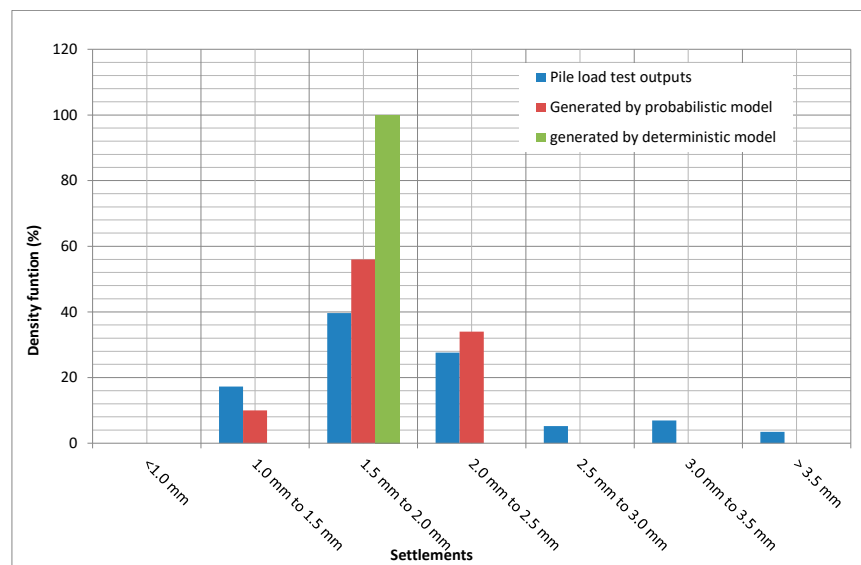


Figure 18. Density functions for generated and pile load test settlement.

So far, the formulated model is a deterministic one in which the same input yields always the same outputs. It is noted that the settlement distribution generated in this way has far less dispersion than the actual pile load test, even though the input data takes into account the soil strength dispersion. A better match is achieved if a probabilistic model is used.

7.4. Model Uncertainty

The fact that the model does not include all the possible variables that intervene in settlement generation but only the main ones can be taken into account by introducing a probabilistic function in the model itself.

The calculation model requires the introduction of a statistical parameter to represent the dispersion of results that is observed in the field.

This statistical parameter is the Z_{peak} factor, which controls the slope of the elastic run on the t-z curves.

The used probabilistic function is the Uniform Density Function whose value is:

$$Z_{\text{peak}} = 0.02 \times \text{Random} + 0.0001 \quad (15)$$

where "Random" is an aleatory number. It varies between 0 and 1. In this way, the Z_{peak} parameter varies uniformly between 0.0001 and 0.02.

The randomness of this parameter reflects the uncertainty of the model in settlement prediction. Its value has been calibrated with usual working load for piles, which on the other hand is where deformations are most interesting.

8. Discussion and Conclusions

This paper develops a numerical model for axially loaded pile which is able to predict its deformation and gives insight about the ultimate skin friction and its distribution along the pile, base resistance and how it is mobilized as loading.

The model is calibrated against sixty two (62) pile load tests carried out on a fairly homogenous soil conditions.

Pile material and piling method are relevant to defined maximum skin friction. In particular, concrete set-in-place shaft resistance has proven to be in the order of 2.0 to 2.5 times greater than metallic piles.

Shear deformation modulus has also been assessed. On the spring model, the shear deformation modulus is related to the slope of the curve t-z, controlled by the Z_{peak} parameter. For concrete piles, Z_{peak} values ranging from 0.25% to 0.17% pile diameter show a good fitting with pile load tests.

In addition, a probabilistic approach helps to understand the uncertainties of the method. Uncertainties due to the measure equipment and soil strength variability have been quantify and represented by their probabilistic functions.

The stochastic variation applied to the input parameters is not enough to simulate the dispersion observed on the pile load test. Therefore, a probabilistic function is also introduced in the model to account for the model uncertainty. Eventually, the generated density function matches in mean and deviation to the pile load test distribution, which means that the model is able to accurately predict settlement and confidence intervals.

Author Contributions: Conceptualization, methodology and investigation, M.B.A., F.E.S.; soft-ware, M.B.A.; review and supervision, E.S.P.; editing, supervision and formal analysis, M.B.A., F.E.S. and E.S.P. All authors have read and agreed to the published version of the manuscript.

Funding: This research received no external funding.

Institutional Review Board Statement: Not applicable.

Informed Consent Statement: Not applicable.

Data Availability Statement: The data presented in this study are available on request from the authors. The data are not publicly available due to they have been gathered and treated for the authors.

Acknowledgments: The authors of the article appreciate the support given in time and resources by Geointec company and the Geology and Research group Geología Aplicada a la Ingeniería Civil of Universidad Politécnica de Madrid.

Conflicts of Interest: The authors declare no conflict of interest.

References

1. Fellin, W. Deep Vibration Compaction as Plastodynamic Problem. Ph.D. Thesis, University of Innsbruck, Innsbruck, Austria, 2000. (In German).
2. Escolano, F.; Bueno, M.; Sánchez, J.R. Interpretation of the pressuremeter test using numerical models based on deformation tensor equations. *Bull. Eng. Geol. Environ.* **2014**, *73*, 141–146. [[CrossRef](#)]
3. Kirsch, F.; Kirsch, K. *Ground Improvement by Deep Vibratory Methods*; CRC Press: Boca Raton, FL, USA, 2016.
4. Massarsch, K.R.; Fellenius, B.H. In situ tests for settlement design of compacted sand. *Proc. Inst. Civil Eng. Geotech. Eng.* **2018**, *172*, 1–11. [[CrossRef](#)]
5. Bueno, M.; Escolano, F.; Sanz, E. Model Uncertainty for Displacement Prediction for Laterally Loaded Piles on Granular Fill. *Appl. Sci.* **2020**, *10*, 613. [[CrossRef](#)]
6. Escolano, F.; Bueno, M.; Sanz, E. Probabilistic Method to Assess Model Uncertainty of Rigid Inclusion on a Granular Fill Supporting a Slab Foundation. *Appl. Sci.* **2020**, *10*, 7885. [[CrossRef](#)]
7. Ditlevsen, O.; Madsen, H.O. *Structural Reliability Methods*; Department of Mechanical Engineering Technical University of Denmark: Kongens Lyngby, Denmark, 2007.
8. American Petroleum Institute. *Geotechnical and Foundation Design Considerations, API RP 2GEO*; American Petroleum Institute: Washington, DC, USA, 2011.
9. Briaud, J.L.; Tucker, L. Piles in sand: A method including residual stresses. *J. Geotech. Eng.* **1984**, *110*, 1666–1680. [[CrossRef](#)]
10. Castelli, F.; Maugeri, M. Simplified nonlinear analysis for settlement prediction of pile groups. *J. Geotech. Geoenviron. Eng.* **2002**, *128*, 76–84. [[CrossRef](#)]
11. Nejad, F.P.; Jaksa, M.B.; Kakhi, M.; McCabe, B.A. Prediction of pile settlement using artificial neural networks based on standard penetration test data. *Comput. Geotech.* **2009**, *36*, 1125–1133. [[CrossRef](#)]
12. Robertson, P.K.; Campanella, R.G. Interpretation of cone penetration tests. Part I: Sand. *Can. Geotech. J.* **1983**, *20*, 718–733. [[CrossRef](#)]
13. Robertson, P.K.; Campanella, R.G.; Wightman, A. Spt-Cpt Correlations. *J. Geotech. Eng.* **1983**, *109*, 1449–1459. [[CrossRef](#)]
14. Puertos del Estado. *Geotechnical Recommendations for the Design of Maritime and Harbour Works*; ROM 0.5/05; Puertos del Estado: Madrid, Spain, 1995.
15. Gibb, H.J.; Holz, W.G. Researche on determining the Density of sand by Spoon Penetration testing. In Proceedings of the 4th International Conference on Soil Mechanics and Foundation Engineering SMFE, London, UK, 12–24 August 1957; pp. 35–39.